Supporting Information

Selective Conversion of Furfural into Tetrahydrofurfuryl Alcohol using Heteropoly acid-based Material as Hydrogenation Catalyst

Paramita Koley[a,b], B. Srinivasa Rao[b], Ylias M. Sabri[a], Suresh K. Bhargava[a] J. Tardio[a*] and N. Lingaiah[b*]

(a) Centre for Advanced Materials & Industrial Chemistry (CAMIC), School of Applied Sciences, RMIT University, GPO BOX-2476, Melbourne 3001, Australia.

(b) Catalysis & Fine Chemicals Division, CSIR-Indian Institute of Chemical Technology, Hyderabad-500 607, India

Chemicals:

All chemicals used in this work were purchased from Sigma-Aldrich A. R. grade (99.9%) to synthesize different catalysts. Different chemicals such as $Na_2MoO_4 \cdot 2H_2O$, $Pd(NO_3)_2 \cdot 2H_2O$, ɣ-Al_2O_3, TiO_2, SiO_2, ZrO_2 and Nb_2O_5 were implemented to prepare different catalysts. The solvents and reagents for example furfural, THFAL, FAL and isopropanol were purchased from both Sigma-Aldrich and Fisher Scientific. Double distilled water was used for the wet impregnation method to synthesize the catalysts.

Raman Spectroscopy:

Fig. S1 represents Raman spectra of $PdMPAV_2$ and supported with various supports like titania, zirconia, alumina, niobia and silica. In $PdMPAV_2$ Raman spectra, a sharp peak at 1000 cm^{-1} related to $M = O_t$ vibration of Keggin ion and two small peak 256 cm^{-1} and 630 cm^{-1} are also Raman characteristic band of MPA Keggin structure[1]. In all supported catalysts the peak at 1000 cm^{-1} was present but the intensity of the peak was poor compared to pure $PdMPAV_2$ as only twenty weight percentage of $PdMPAV_2$ was loaded in the oxide support. For the alumina supported catalysts the broad peak at 430 cm^{-1} is corresponds to α-Al_2O_3[2]. Zirconia supported catalyst also exhibited the main characteristic peaks of ZrO_2 at 486 cm^{-1} and 658 cm^{-1}[1]. Moreover, the Raman profile of $PdMPAV_2/SiO_2$ mainly contained the peak at 500 cm^{-1} which belong to SiO_2[3]. The broad peak at 700 cm^{-1} for Raman profile of niobia supported catalyst represented to the characteristic peak of niobia. For titania supported catalyst the three

main peaks at 380 cm^{-1}, 540 cm^{-1} and 750 cm^{-1} are related to anatase phase of titania[4]. The Raman spectra of all supported catalysts mainly contained the peaks corresponds to the characteristic peak of the support material.

Determination of Metal dispersion, Surface Area and Particle size by Chemisorption:

The metal dispersion factor in a metal catalyst which is supported with different supports are generally described as the proportional ratio of the total number of surface atoms and the total number of atoms in the catalyst. This ranges of this factor is from 0 to 1, where 1 correlated to the atomic level dispersion of the metal on the catalyst support (most of the cases it may not achieve unity).[5, 6] The normalized equations to measure the metal dispersion, active metal surface area and metal crystallite size are provided bellow:

$$\text{Dispersion (\%)} = \frac{Uptake\ (\frac{\mu mol}{gcat})}{Total\ metal\ (\frac{\mu mol}{gcat})} \times 100$$

Metal area = Metal cross sectional area × No. of metal atoms on surface

$$\text{Particle size (nm)} = \frac{6000}{total\ metal\left(\frac{m2}{gcat}\right) \times \rho\ (\frac{g}{cc})}$$

ρ = metal density

Product Analysis by Gas Chromatography (GC/GC-MS):

All the reactants, products and intermediate are confirmed and analyzed by GC-MS (Model QP 5050 supplied by M/S. Shimadzu Instruments Corporation, Japan) and GC (Shimadzu 2010) respectively. The GC is equipped with flame ionization detector (FID) and INNO Wax capillary column (diameter: 0.25 mm, length: 30 m) is used for the separation of the reaction mixtures. The product and reactant mixture which are collected from the reactor was added into the organic solvents (methanol or acetone) and equal amount of an internal standard (anisole) was added before starting the GC analysis. The GC programming conditions are different for different reactions. The temperature of the injector is 250 °C, the temperature of oven/column is usually 80 – 280 °C with the ramping rate of 10 °C min^{-1} and holding time is

3 and 5 minutes for starting and the end time of the analysis respectively. The FID temperature is 300 ℃.

The conversion of reactant=$\left(\frac{Furfuralc_{intial} - Furfuralc_{final}}{Furfuralc_{intial}}\right) \times 100$

Selectivity of the product=$\left[\frac{P_i}{\sum P_i}\right] \times 100$ (where i= product, reactant and intermediate for particular reaction and P is targeted product.) where reactant is furfural.

Yield=$\left(\frac{Conversion \times Selectivity}{100}\right)$

The carbon balance was attained by calculating the amount of carbon in liquid phase reaction by GC-FID and measured by the equation,[7]

Carbon balance (%) = $100 \times \frac{(moles\ of\ carbon\ out\ (all\ products\ and\ reactants))}{moles\ of\ carbon\ in\ (reactant)}$

Here reactant is furfural. Products are THFAL, FAL, MeTHF, MeF and 1,5 pentanediol which mainly depends on reaction condition and catalysts.

The initial turn over frequency (TOF) of the catalyst was calculated by this equation.

TOF = $\frac{(moles\ of\ product)}{\{(moles\ of\ metal\ in\ catalyst)\ \times (dispersion)\ \times (reaction\ time)\}}$

The product mentioned in the equation is the targeted product, THFAL.

Hot Filtration Test:

A hot filtration test was also investigated to determine the heterogenicity of the catalyst under the optimized reaction condition. 100 ml Parr Autoclave was pressurized with 2.5 H_2 pressure and loaded with furfural (2 .402 wt.%), catalyst (0.8 wt.%) and 25 ml isopropanol and set the reaction temperature at 150 ℃. After one hour of reaction, the catalyst was filtered and

separated from the reaction solution; furthermore, the reaction was carried out for 2 h. The yield of THFAL was not enhanced which is confirmed by GC-MS analysis. It can be interpreted that this catalyst is reusable as well as stable for this reaction without leaching of the metal. The tests confirmed that the catalyst was stable and reusable under the reaction condition.

Recyclability tests:

After the completion of the reaction the catalyst was washed with MeOH with two or three times and dried in 60 ℃ oven for overnight. After that the catalyst was employed for the next catalytic cycle. The conversion and the selectivity of the reactant and products after the reaction were analyzed by GC.

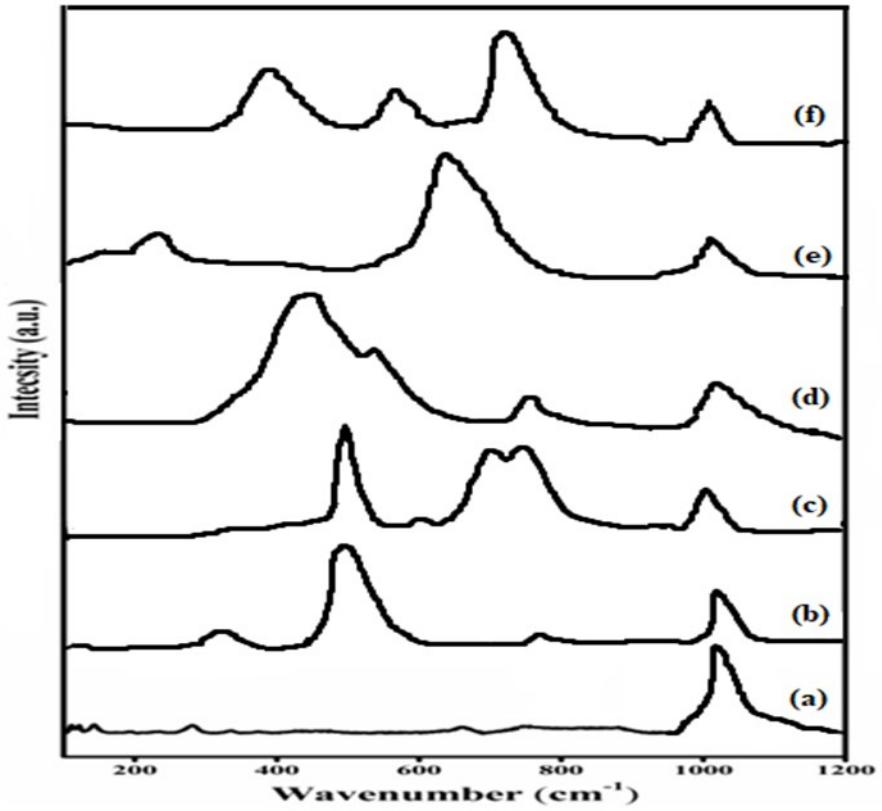

Fig. S1: Raman profiles of palladium exchanged vanadium incorporate molybdophosphoric acid on different supports. (a) $PdMPAV_2$ (b) $PdMPAV_2/Al_2O_3$ (c) $PdMPAV_2/ZrO_2$ (d) $PdMPAV_2/SiO_2$ (e) $PdMPAV_2/Nb_2O_5$ (f) $PdMPAV_2/TiO_2$

Table S1: Surface area of supports

Support	Surface area (m^2g^{-1})
Al_2O_3	100
ZrO_2	75
TiO_2	80
Nb_2O_5	60
SiO_2	395

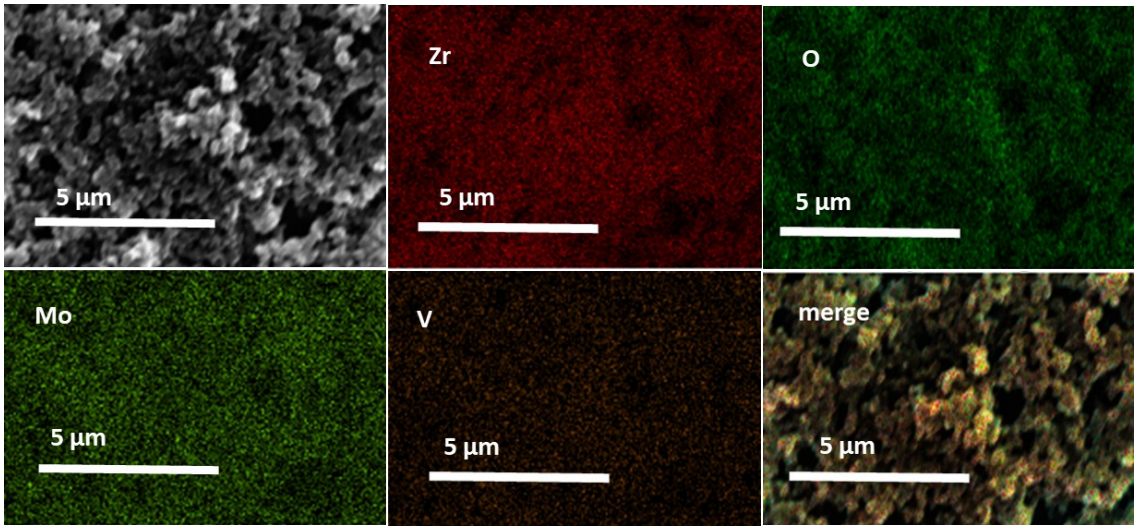
5 µm
Zr
5 µm
O
5 µm
Mo
5 µm
V
5 µm
merge
5 µm

(a)

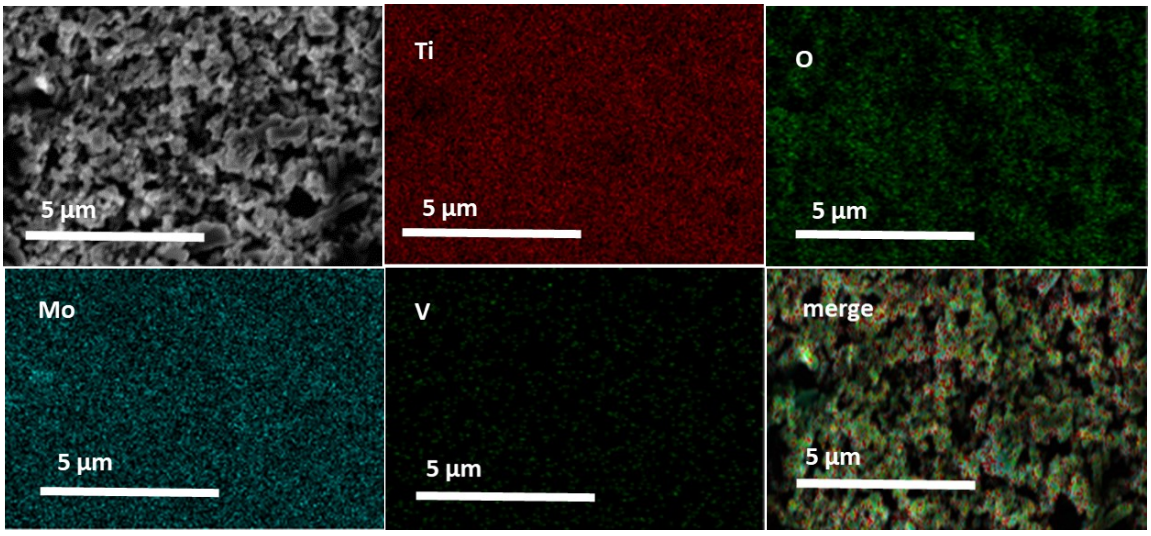
5 µm
Ti
5 µm
O
5 µm
Mo
5 µm
V
5 µm
merge
5 µm

(b)

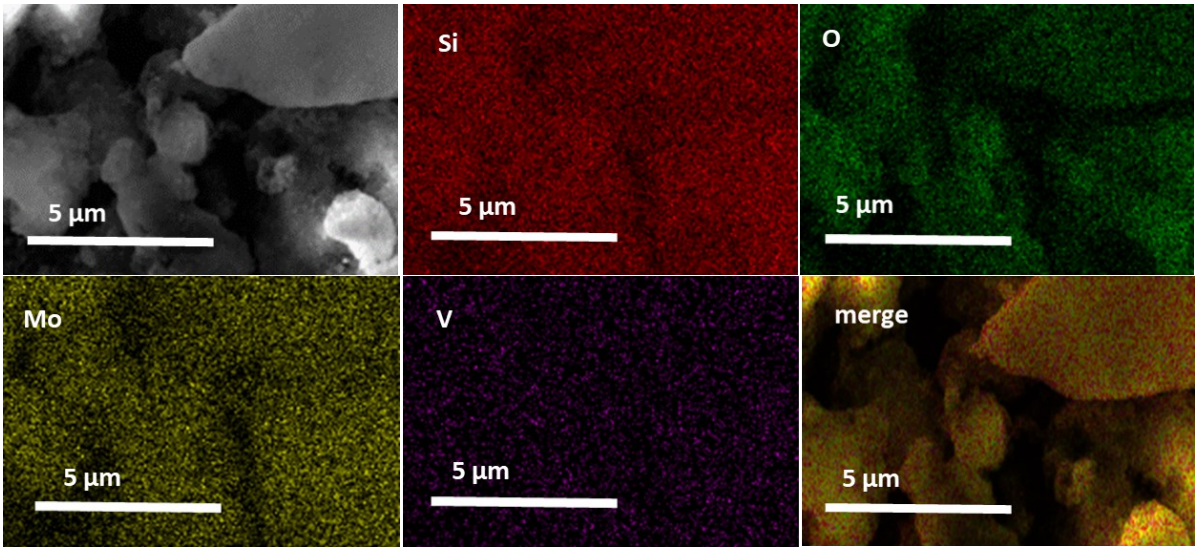
5 µm
Si
5 µm
O
5 µm
Mo
5 µm
V
5 µm
merge
5 µm

(c)

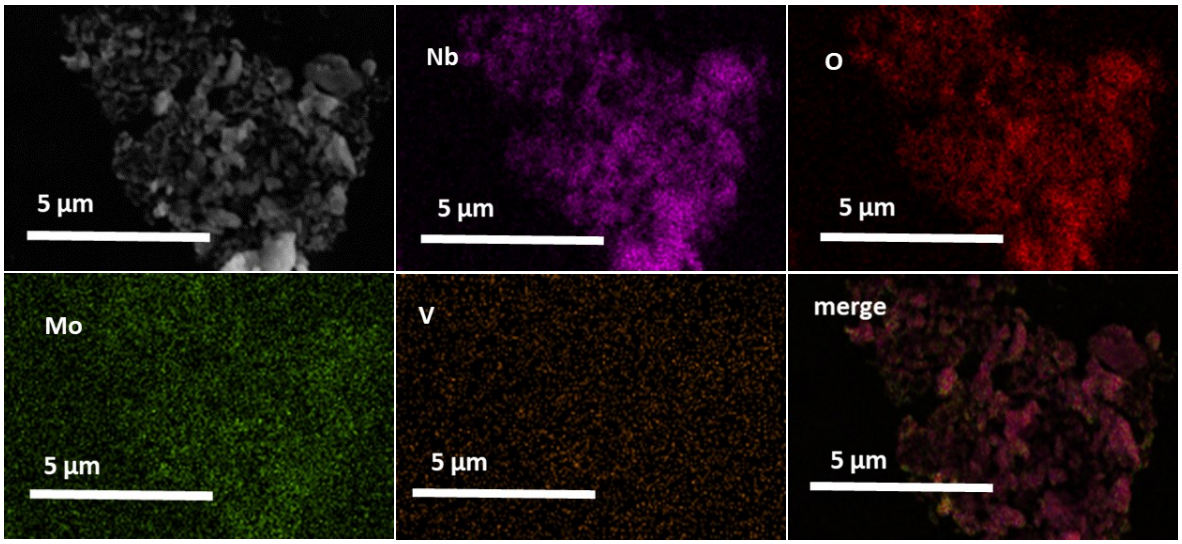

(d)

Fig. S2: Elemental mapping of (a) $PdMPAV_2/ZrO_2$ (b) $PdMPAV_2/TiO_2$ (c) $PdMPAV_2/SiO_2$ (d) $PdMPAV_2/Nb_2O_5$

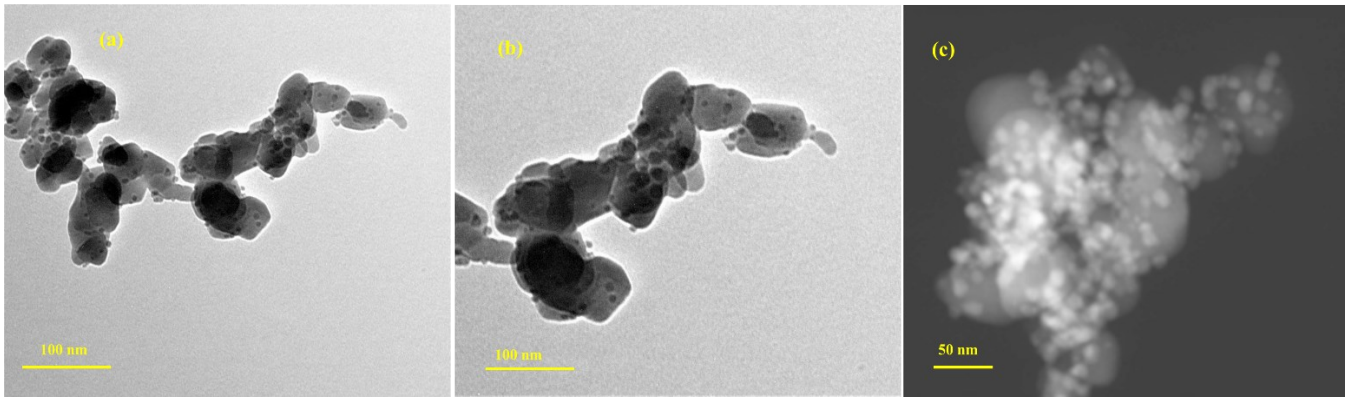

Fig S3: (a) & (b) TEM and (c) STEM of $PdMPAV_2/Al_2O_3$

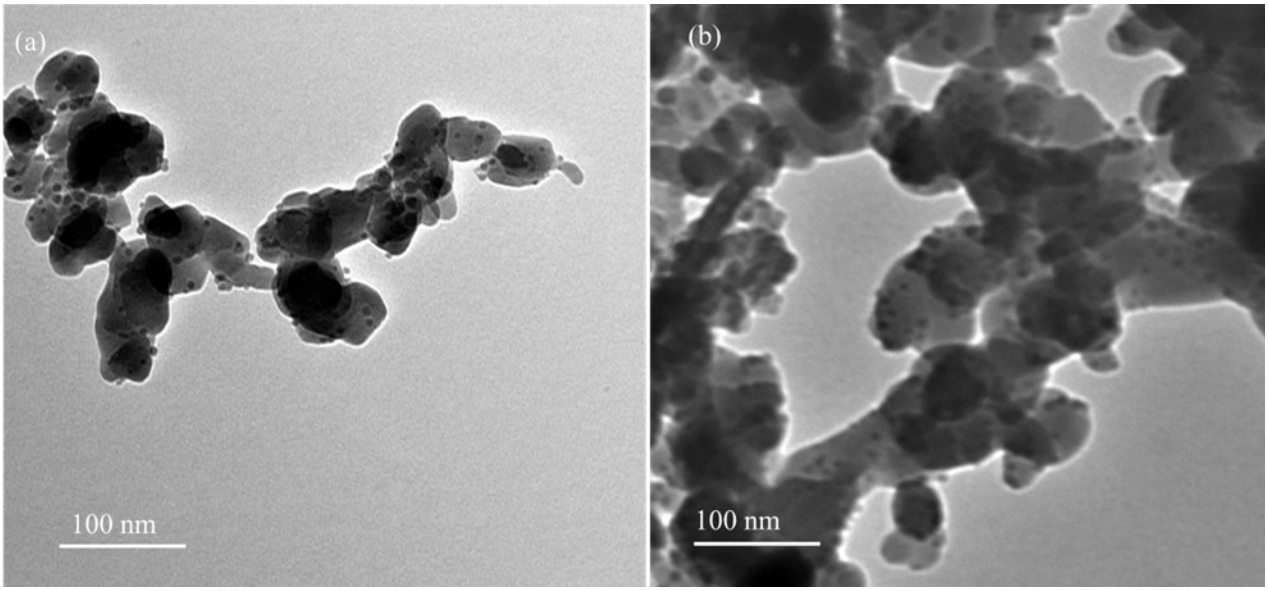

Fig. S4: TEM images of (a) fresh $PdMPAV_2/Al_2O_3$ (b) used $PdMPAV_2/Al_2O_3$

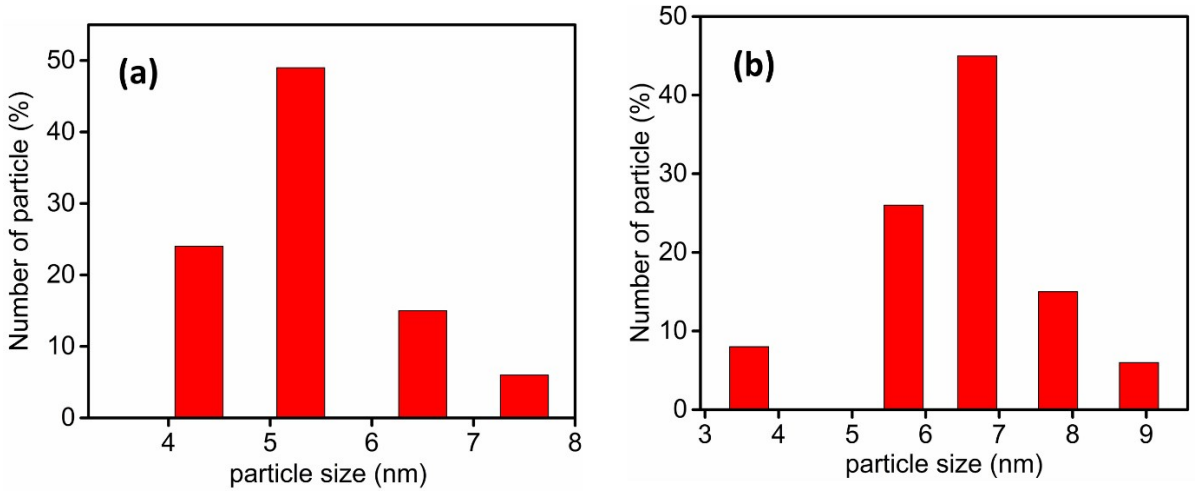

Fig.S5: Particle size distribution of (a) Fresh $PdMPAV_2/Al_2O_3$ and (b) used $PdMPAV_2/Al_2O_3$ catalyst.

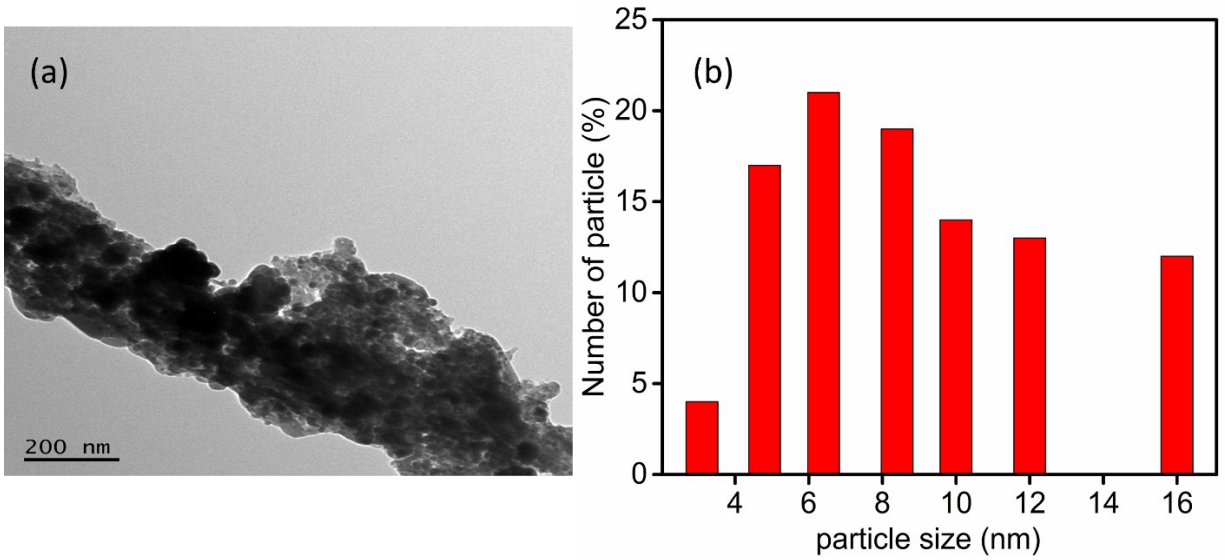

Fig. S6: (a) TEM image of Pd/Al_2O_3 catalyst (b) particle size obtained from TEM

Table S2: Activity of different catalysts

Catalyst	Furfural Conversion (%)	THFAL selectivity (%)	FAL selectivity (%)	MeTHF selectivity (%)	MeF selectivity (%)	1,5 pentanediol selectivity (%)	Carbon balance (%)
Pd/Al_2O_3	65	68.50	22.30	0	0.08	9.12	98.4
$Pd\text{-}V/Al_2O_3$	67.1	66.34	26.06	0	0	7.60	97.6
$PdMPA/Al_2O_3$	81.8	80	8	0	0	12	98.2
$PdMPAV_1/Al_2O_3$	87.1	88.3	7.7	0	0	4	98.1
$PdMPAV_2/Al_2O_3$	100	95	0	5	0	0	98.3

Table S3: CO-chemisorption studies

Different catalyst	Active metal surface area (m^2g^{-1})	Dispersion factor (%)	Metal Particle Diameter (nm)
Pd/Al_2O_3	42.5	15.7±3.5	7.2
$Pd\text{-}V/Al_2O_3$	43.6	17.5±3.6	7.0
$PdMPA/Al_2O_3$	62.1	23.5±3.6	6.4
$PdMPAV_1/Al_2O_3$	69.2	27.8±3.4	6.3
$PdMPAV_2/Al_2O_3$	75.8	33.8±3.8	5.3

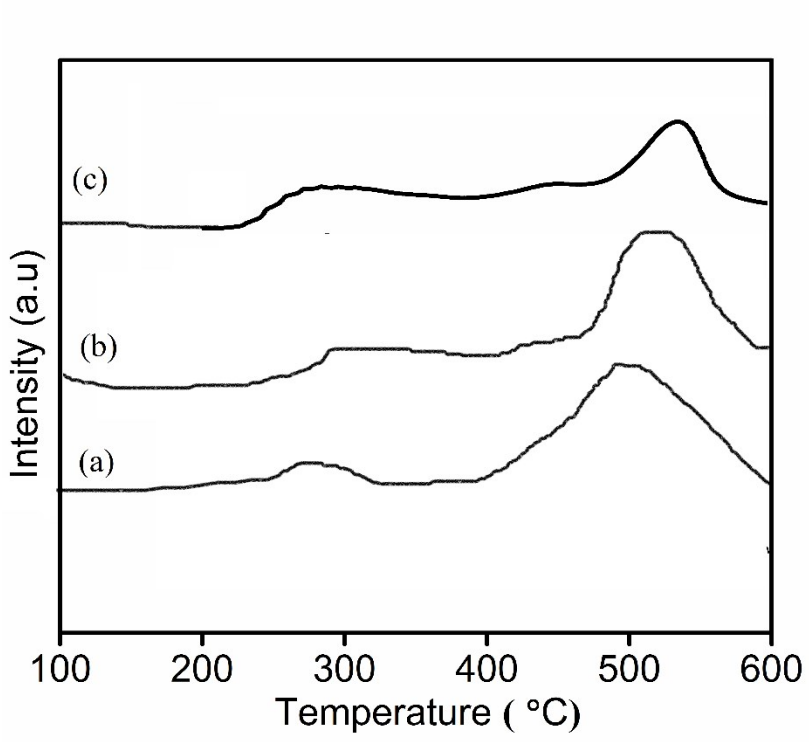

Fig S7: NH_3-TPD of (a) $PdMPA/Al_2O_3$ (b) $PdMPAV_1/Al_2O_3$ (c) $PdMPAV_2/Al_2O_3$

Table S4: Acidity obtained from NH_3-TPD results

Different catalyst	Total acidity (mmol g^{-1})
$PdMPA/Al_2O_3$	1.543
$PdMPAV_1/Al_2O_3$	1.312
$PdMPAV_2/Al_2O_3$	1.214

Table S5: Comparison of $PdMPAV_2$-Al_2O_3 catalyst with previously reported catalysts

Catalyst	Reaction time (h)	Temperature (°C)	H_2 Pressure (MPa)	Solvent	Furfural conversion (%)	FAL Conversion (%)	THFAL Yield (%)	TOF (h^{-1})	THFAL yield $g_{catalyst}^{-1}$	Reference
Pd/MFI (3 wt% Pd)	5	220	3.4	isopropanol	93	-	83	14	65.4	[8]
Ni/g-Al_2O_3 (15 wt% Ni)	2	80	4	Ethanol	-	99.8	99.5	24	87.6	[9]
Pd–Ir–ReO_x/SiO_2	2	50	6	water	>99.9	-	78	30.7	130.3	[10]
Ni/C-500 (derived from MOF)	2	120	1	2-propanol	100	-	99	28.4	120.7	[11]
Rh/C (5 wt% Rh	32	30	1	N, N-dimethylacetamide (DMA)	96	-	95	30	121.2	[12]
	16	30	0.1	DMA	-	100	96	31	123	
Ni–Co/SBA-15	2	90	5	Ethanol			92	20.3	89.0	[13]
Pd–Ir–ReO_x/SiO_2	8	40	6	water	99.9		66.8	30	78.9	[14]
Pt-Li/Co_2AlO_4	24	130	1.5	ethanol			31.3%	8	45.8	[15]
$PdMPAV_2/Al_2O_3$ (0.5 wt.% Pd)	6	150	2.5	isopropanol	100	-	95	32.6	118.7	This work
	2	150	1.5	isopropanol	-	100	100	33.7	125	This work

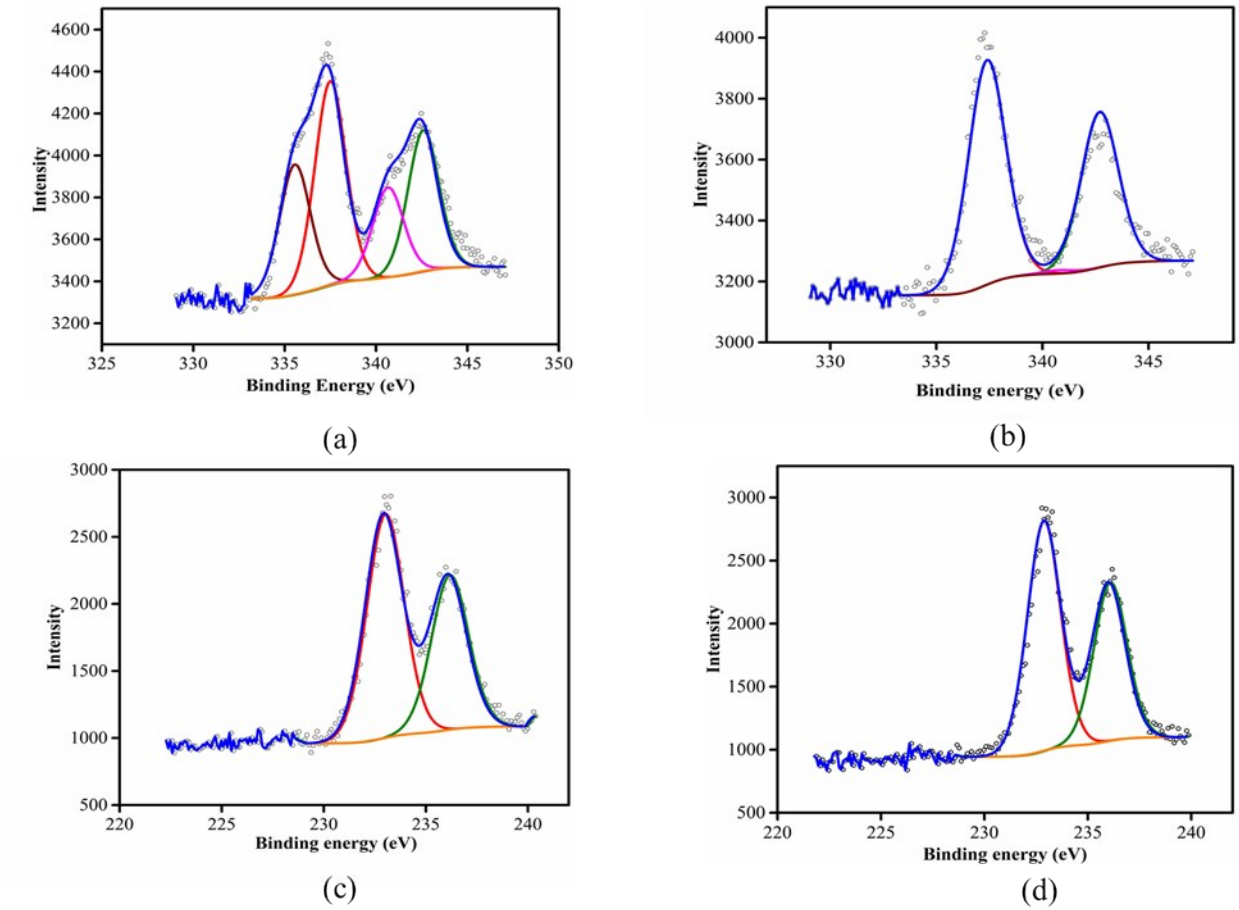

Fig. S8: XPS spectra of $PdMPAV_2$-Al_2O_3 (a) Pd-3d for reduced (b) Pd-3d for fresh (c) Mo-3d for reduced (d) Mo-3d for fresh

Table S6: Binding energy values of V and Al

Catalyst	Al $2p_{3/2}$ (e.V)	V $2p_{3/2}$ (e.V)
Reduced catalyst $PdMPAV_2/Al_2O_3$	74.8	517.9
Catalyst before reduction $PdMPAV_2/Al_2O_3$	74.5	517.9

Table S7: Carbon balance for effect of temperature, pressure, time and catalyst concentration

Effect of time		Effect of temperature		Effect of H_2 Pressure		Effect of catalyst concentration		Effect of initial concentration of furfural	
Time (h)	Carbon balance (%)	Temperature (°C)	Carbon balance (%)	H_2 pressure	Carbon balance (%)	Catalyst concentration (wt.%)	Carbon balance (%)	Furfural initial conc. (wt.%)	Carbon balance (%)
2	98.6	90	98.6	1	98.7	0.4	98.5	1.2	98.5
4	98.4	120	98.5	1.5	98.4	0.6	98.6	2.4	98.3
6	98.3	150	98.3	2	98.3	0.8	98.3	3.6	98.1
8	98.3	180	98.0	2.5	98.1	1	98.1	4.8	95.6
-	-	200	95.3	3	98.3	1.2	98.1	6.0	94.3

Table S8: Carbon balance in recyclability tests

No of cycles	Carbon balance (%)
1	98.3
2	98.1
3	98.3
4	97.9
5	98.1

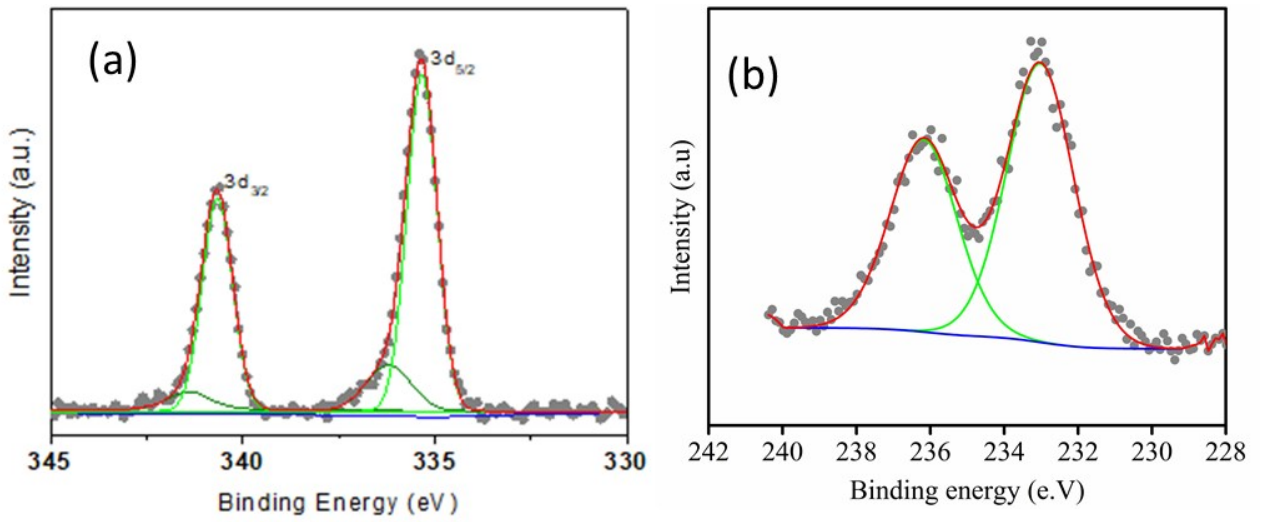

Fig. S9: XPS of (a) Pd-3d (b) Mo-3d for used $PdMPAV_2$-Al_2O_3 catalyst

Table S9: Binding energy values of used $PdMPAV_2$-Al_2O_3 catalyst

Catalyst	V 2p (e.V)	O 1s (e.V)	P 2p (e.V)	Al 2p (e.V)
Used $PdMPAV_2$-Al_2O_3	517.7	531.8 530.7	134.7	74.7

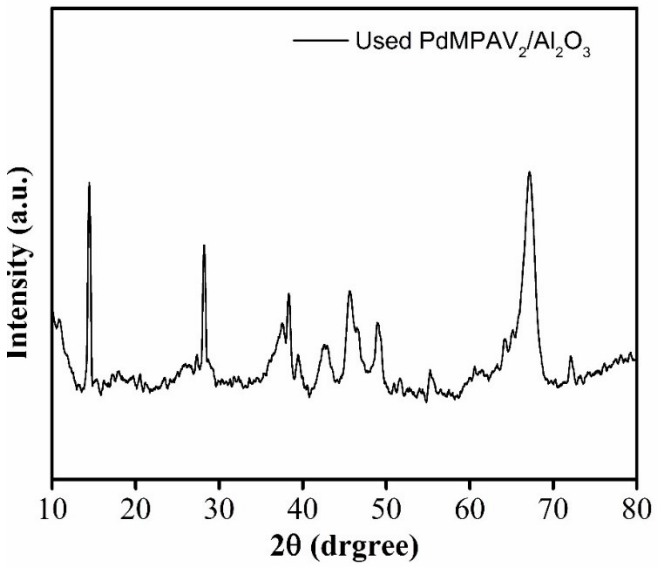

Fig. S10: XRD of used $PdMPAV_2$-Al_2O_3 catalyst

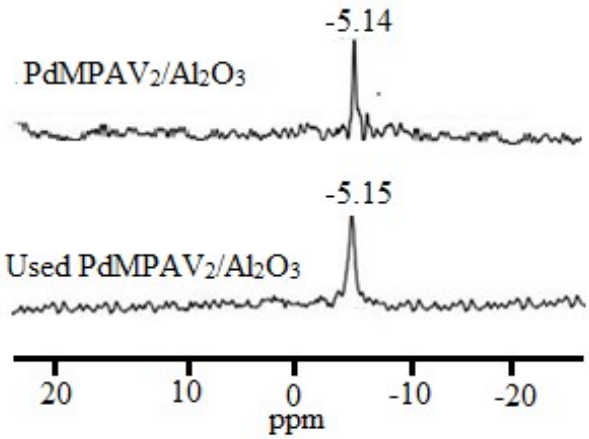

Fig. S11: ^{31}P NMR of $PdMPAV_2$-Al_2O_3 and Used $PdMPAV_2$-Al_2O_3 catalyst

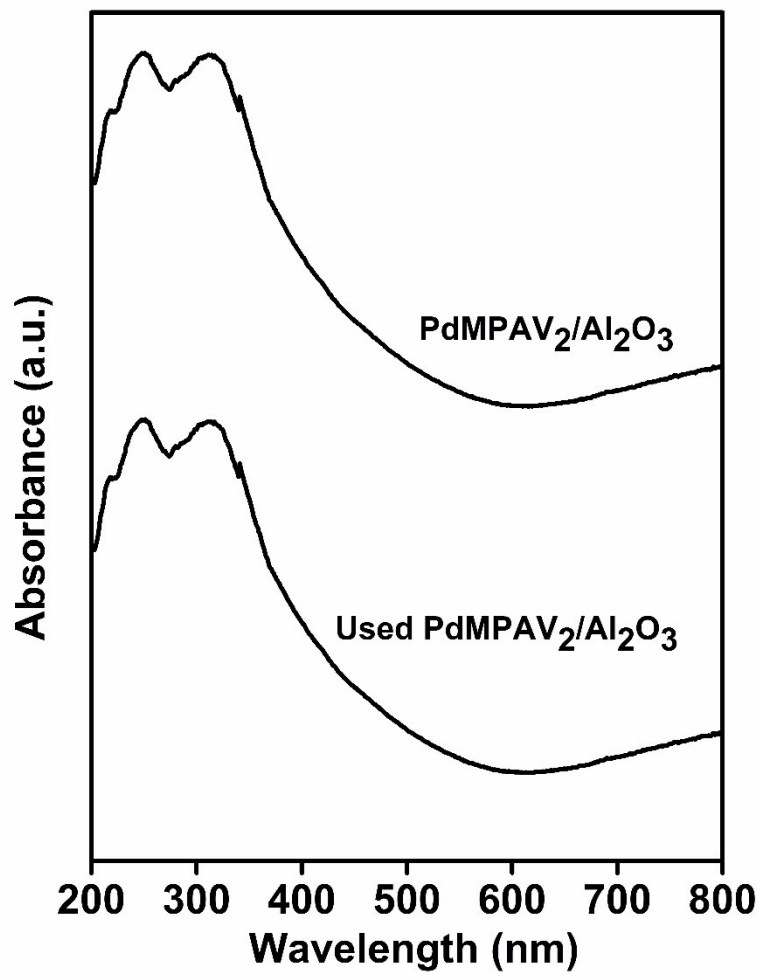

Fig. S12: UV visible spectra of $PdMPAV_2$-Al_2O_3 and Used $PdMPAV_2$-Al_2O_3 catalyst

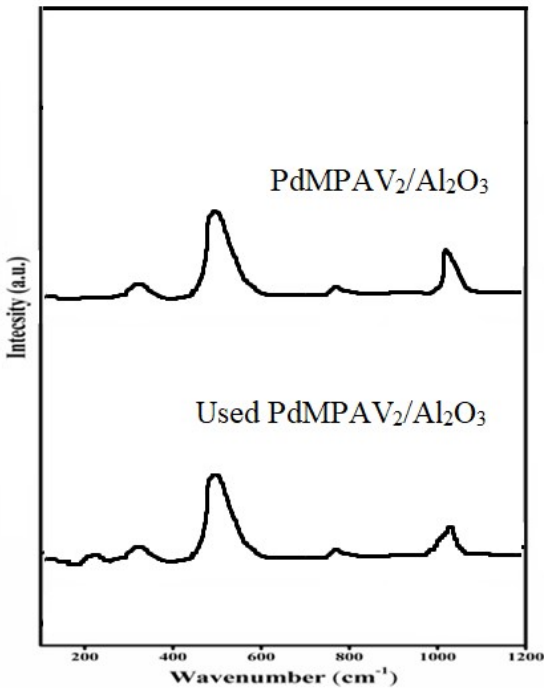

Fig. S13: Raman spectra of $PdMPAV_2$-Al_2O_3 and Used $PdMPAV_2$-Al_2O_3 catalyst

References

1. K. V. Rao, P. Rao, P. Nagaraju, P. S. Prasad and N. Lingaiah, *Journal of Molecular Catalysis A: Chemical*, 2009, **303**, 84-89.
2. J. Gangwar, B. K. Gupta, S. K. Tripathi and A. K. Srivastava, *Nanoscale*, 2015, **7**, 13313-13344.
3. G. Dovbeshko, O. Fesenko, V. Boyko, V. Romanyuk, V. Moiseyenko, V. Gorelik, L. Dolgov, V. Kiisk and I. Sildos, 2012.
4. H. A. Mahmoud, K. Narasimharao, T. T. Ali and K. M. Khalil, *Nanoscale research letters*, 2018, **13**, 48.
5. I. Langmuir, *Journal of the American Chemical society*, 1918, **40**, 1361-1403.
6. I. Langmuir, *Journal of the American chemical society*, 1916, **38**, 2221-2295.
7. J. Lee, Y. Xu and G. W. Huber, *Applied Catalysis B: Environmental*, 2013, **140**, 98-107.
8. N. S. Biradar, A. M. Hengne, S. N. Birajdar, P. S. Niphadkar, P. N. Joshi and C. V. Rode, *ACS Sustainable Chemistry & Engineering*, 2014, **2**, 272-281.

9. S. Sang, Y. Wang, W. Zhu and G. Xiao, *Research on Chemical Intermediates*, 2017, **43**, 1179-1195.
10. S. Liu, Y. Amada, M. Tamura, Y. Nakagawa and K. Tomishige, *Green Chemistry*, 2014, **16**, 617-626.
11. Y. Su, C. Chen, X. Zhu, Y. Zhang, W. Gong, H. Zhang, H. Zhao and G. Wang, *Dalton Transactions*, 2017, **46**, 6358-6365.
12. B. M. Matsagar, C.-Y. Hsu, S. S. Chen, T. Ahamad, S. M. Alshehri, D. C. Tsang and K. C.-W. Wu, *Sustainable Energy & Fuels*, 2020, **4**, 293-301.
13. S. Li, Y. Wang, L. Gao, Y. Wu, X. Yang, P. Sheng and G. Xiao, *Microporous and Mesoporous Materials*, 2018, **262**, 154-165.
14. Y. Nakagawa, M. Tamura and K. Tomishige, *Catalysis Surveys from Asia*, 2015, **19**, 249-256.
15. R. Karinen, K. Vilonen and M. Niemelä, *ChemSusChem*, 2011, **4**, 1002-1016.